Pulsed infrared laser annealing of gold nanoparticles embedded in a silica matrix

A. Halabica,[1,a)] J. C. Idrobo,[1,b)] S. T. Pantelides,[1,b)] R. H. Magruder III,[2] S. J. Pennycook,[3,c)] and R. F. Haglund, Jr.[1]

[1]*Department of Physics and Astronomy, Vanderbilt University, 6301 Stevenson Center, Nashville, Tennessee 37235, USA*

[2]*Department of Chemistry and Physics, Belmont University, 1900 Belmont Blvd., Nashville, Tennessee 37212, USA*

[3]*Materials Science and Technology Division, Oak Ridge National Laboratory, P.O. Box 2008, Oak Ridge, Tennessee 37831, USA*

(Received 30 January 2008; accepted 6 March 2008; published online 28 April 2008)

Pulsed infrared laser irradiation was used to modify the optical and physical properties of gold nanoparticles in a SiO_2 substrate. The primary laser wavelength used for annealing was 8 μm, where the primary absorption was in the substrate. The optical absorption spectra exhibit a typical surface plasmon peak at 520 nm, which increases with laser fluence. This implies growth of the gold nanoparticles during laser annealing but the size distribution remains narrow, unlike some thermal annealing procedures that produce bimodal size distributions. The results were confirmed by scanning transmission electron microscopy and were consistent with the calculations of expected extinction spectra. © *2008 American Institute of Physics*. [DOI: 10.1063/1.2909965]

I. INTRODUCTION

Nanocomposite materials comprised of metal nanoparticles embedded in a dielectric matrix have potential applications based on their enhanced third-order optical nonlinearity.[1] These materials have been fabricated by alternating deposition metal and dielectric matrix layers,[2] cosputtering,[3] ion exchange,[4] and ion implantation.[1] Laser annealing is one of the postprocessing techniques used to modify the nanocomposite and its effects on the composite materials have been extensively studied.[5–11] The laser wavelength, fluence, and pulse duration are the usual variable parameters of the laser annealing experiments. In most previous experiments, the laser wavelength is in a spectral region where the dielectric matrix is transparent so that the laser light is primarily absorbed by the metal nanoparticles. There are also several experiments[6,9,11,12] that make use of matrix absorption in the ultraviolet (UV). However, there are no reported experiments on the effects of laser light on the infrared (IR) absorption region of the dielectric matrices.

In this study, we report successful IR laser annealing of nanocomposites consisting of Au nanoparticles embedded in a fused-silica matrix. The experiments demonstrate the unique effects of fast thermal heating of the matrix on the size and size distribution of embedded metal nanocrystals, using photons with energies far below the bulk bandgap of the matrix. We find that the ambient environment has no influence on the IR laser-induced ripening. The process differs from that found in UV laser annealing of transparent substrates, where most of the laser energy is absorbed by the nanoparticles and the nanoparticle ripening is assisted by free-electron heating. Also, in the case of silicate glasses,[13] where there is a strong matrix absorption of UV light, the primary interaction is nonthermal, such as electron-hole pair creation, followed by thermalization processes. However, what we have demonstrated is a true rapid thermal annealing, where the nanocomposite material is fully in thermal equilibrium. This opens the door to direct writing of waveguides and other interesting structures in metal-silica nanocomposites. In addition, since the optical penetration depth in fused silica is a strong function of wavelength in the 7–10 μm region, this technique can also be used to control annealing depth in these nanocomposites[14,15]

II. EXPERIMENT

In our experiments, Corning 7940, type III fused-silica substrates were implanted with 1.1 MeV Au^+ ions at Oak Ridge National Laboratory using a tandem implanter. The substrate was held at 400 °C during implantation and the current densities were maintained below 15 μA. The ion dose was 6×10^{16} ions/cm^2. The projected and longitudinal straggling ranges that were calculated using SRIM 2003 program were 267 and 36 nm, respectively. The Vanderbilt Mark-III free-electron laser[16] (FEL) was used to anneal the samples at different fluences. The FEL is tunable in the mid-IR from 2 to 10 μm and the mode structure of the beam is TEM_{00}. The pulse frequency is 30 Hz. Each pulse is about 4 μs long and is composed of a train of picosecond pulses separated by approximately 350 ps. The metal implanted layer was well within the $1/e$ absorption length for SiO_2 ($\sim$3.4 μm) at 8 μm wavelength. Optical absorption spectroscopy and scanning transmission electron microscopy (STEM) were used to characterize the samples. The Mie theory was used to fit the optical spectra, and thus, obtained

a)Electronic mail: andrej.halabica@vanderbilt.edu.

b)Also at Materials Science and Technology Division, Oak Ridge National Laboratory, Oak Ridge, Tennessee 37831, USA.

c)Also at Department of Physics and Astronomy, Vanderbilt University, 6301 Stevenson Center, Nashville, Tennessee 37235, USA.

 © 2008 American Institute of Physics

Downloaded 15 Aug 2008 to 160.91.172.37. Redistribution subject to AIP license or copyright; see http://jap.aip.org/jap/copyright.jsp

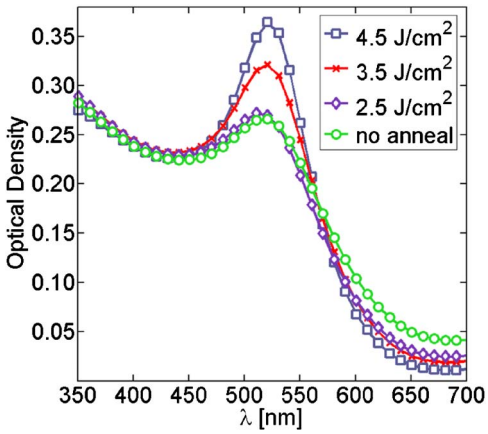

FIG. 1. (Color online) Optical absorption spectra of the Au implanted samples that are laser annealed at different fluences.

particle size data were compared to STEM data where these were available.

The FEL beam was scanned across the surface of the sample at approximately 1 mm/s with an angle of incidence of 45°. A CaF_2 lens with a focal length of 500 mm was used for focusing. The spot diameter at the surface was ~300 μm which allows for a good overlap of two consecutive macropulses. The energy per pulse used for annealing was in the range from 5 to 9 mJ, which corresponds to a fluence range of 2.5–4.5 J/cm^2. All optical absorption spectra were measured with a Cary 5000 UV-visible-near-IR dual-beam spectrophotometer in the 200–800 nm wavelength range with an analyzing beam of 5 mm in diameter. The samples were also characterized using 1.8 MeV He^+ Rutherford backscattering spectrometry (RBS). The backscattering collection angle was 175° and the collected charge was 3 μC. The energy resolution was 22 keV and the beam current was kept under 10 nA. The RBS data were normalized to channel 200 in order to compensate for variations in surface charging effects from sample to sample. STEM was performed at the Oak Ridge National Laboratory using 300 kV (VG microscopes) HB603U scanning transmission electron microscope equipped with aberration corrector (Nion Co.).

III. RESULTS AND DISCUSSION

Figure 1 (Ref. 7) shows the optical absorption spectra of the Au implanted samples after laser annealing at different pulse energies. With increasing fluence, the intensity of the surface plasmon resonance peak at 520 nm increases. This increase is similar to that observed in thermal annealing experiments[17] attributed to the increase in the mean particle diameter. The effects of the IR pulsed laser annealing, while similar to the effects of furnace annealing in air, are not dependent on atmosphere whereas conventional thermal annealings are very dependent on annealing atmosphere.

To test the influence of the atmosphere, we performed a simple experiment wherein two pieces of the Au implanted sample were laser annealed, one in air and the other in vacuum (4×10^{-2} Torr). The resulting optical spectra were identical, which leads to the conclusion that the IR laser annealing is not affected by the surrounding atmosphere. A possible explanation is that the pulsed laser annealing is so fast (4 μs/macropulse) that there is insufficient time for the atoms or molecules present in the atmosphere to diffuse into the matrix and influence the processes that are taking place there.

During laser annealing, the pulse energy is deposited into the near-surface layer whose thickness depends on the laser wavelength and the absorption coefficient of the matrix material at that wavelength. For silica, there is a significant absorption both in the UV and IR regions of the spectrum. There have been numerous studies investigating the effects of excimer (UV) laser pulses on metal-glass composites. In those cases, the coupling mechanism of the laser light is through excitation of bound electrons into the conduction band and subsequent free-electron heating. The overall effect of intense excimer laser pulse is the heating of the surface layer following the absorption of the UV laser light in the matrix and also the metal nanoparticles.[12]

The laser wavelength used in our experiment was 8 μm, well within the mid-IR absorption region of fused silica which starts at a wavelength around 6 μm and peaks at 9.6 μm. The coupling is thermal since the energy of 8 μm wavelength photons is close to the excitation energy of the Si–O bond vibrational mode. Moreover, the macropulse duration is comparable to the thermal diffusion time (~14 μs) (Ref. 20) for fused silica so that the condition for thermal confinement of the laser energy is more or less satisfied. From the energy of the pulse and the basic thermal parameters of the silica matrix, it is possible to make a simple estimate of the surface temperature during laser annealing. For the used maximum pulse energy (9 mJ), the estimated temperature (~2250 K) is higher than the softening point of the fused silica (1958 K) and is significantly higher than the temperatures used in furnace annealing.[17] However, high temperature is only present in the near-surface layer and is rapidly quenched due to heat diffusion. For the estimated temperature rise of ~1950 K within the pulse duration of 4 μs, the heating rate is 4.9×10^8 K/s. Nanoparticle melting is expected since the bulk gold (1340 K) melting temperature is lower than the estimated temperature rise in the silica surface layer and the melting temperature of the nanoparticles is even lower than the bulk melting temperature due to thermodynamic size effects.[18] The temperature at which the Au particles and possibly also silica matrix melt, together with fast heating and cooling rates, allows rapid diffusion of the Au atoms implanted in the near-surface layer. Even though such conditions last for only a very short time after the laser pulse, the time is evidently sufficient to cause significant growth of the Au nanoparticles, which is similar to the growth that occurs during furnace annealing in air.[17]

RBS measurement was used to study the effects of IR laser annealing on the depth distribution of implanted Au ions. The data show that laser treatment has no effects on the depth profile or on the amount of Au inside the matrix, which is in agreement with the fact that the Au diffusivity in SiO_2 is low.[22] Using a simple backscattering analysis,[21] the projected

Downloaded 15 Aug 2008 to 160.91.172.37. Redistribution subject to AIP license or copyright; see http://jap.aip.org/jap/copyright.jsp

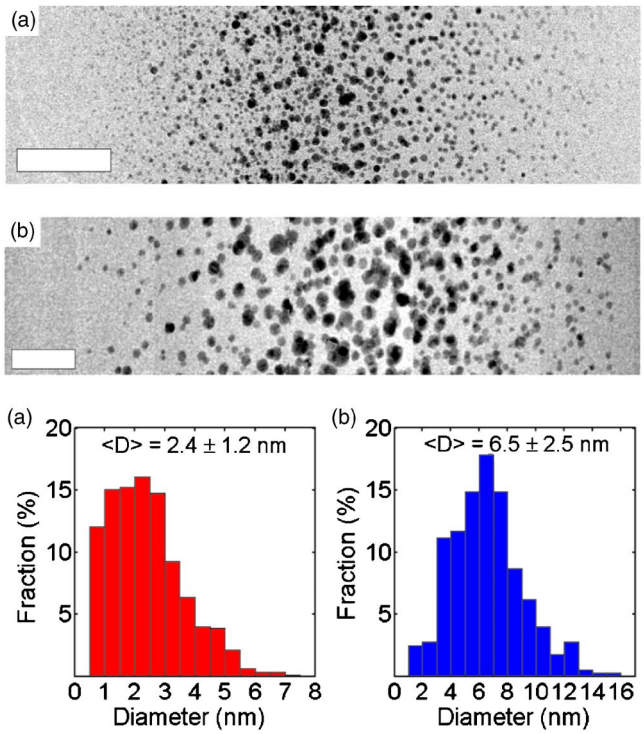

FIG. 2. (Color online) Cross-sectional bright-field STEM images (scale bar=50 nm) and the cluster size distributions of (a) the as-implanted sample and (b) the FEL annealed sample (fluence=4.5 J/cm^2).

range was calculated for as-implanted sample to be 260 nm and for the 4.5 J/cm^2 annealed one to be 252 nm. These results agree well with the value of 267 nm calculated by SRIM, noting that the calculation did not include surface sputtering.

Figure 2 shows the STEM images and the Au cluster size distributions of the as-implanted sample [Fig. 2(a)] and the IR pulsed laser annealed (fluence=4.5 J/cm^2) sample [Fig. 2(b)]. The average cluster size changes from $\langle D\rangle = 2.4 \pm 1.2$ nm for the as-implanted sample to $\langle D\rangle = 6.5 \pm 2.5$ nm for the laser annealed one. Another thing to notice is that the cluster density was significantly reduced (approximately five times) by the annealing process. This suggests that the smaller size particles dissolve into the matrix and then contribute to the growth of the larger clusters. A similar process was observed in the thermal annealing experiments performed in air atmosphere.[23] Interestingly, the width of the size distribution that is stated as a fraction of the average diameter actually narrows in the FEL annealed sample, in contrast to what one usually observes during the conventional thermal annealing.

A nonlinear fit to the optical spectra was employed to extract the average diameter in comparison with the STEM analysis by using the procedure of Miotello *et al.*[17] The definition of the optical density

$$\mathrm{OD}(\omega) = A\int_0^\infty dR f(R)\sigma(R,\omega) \tag{1}$$

was used as the fitting function, where the constant A is proportional to the particle concentration and the thickness of the implanted layer. The extinction cross-sectional $\sigma(R,\omega)$

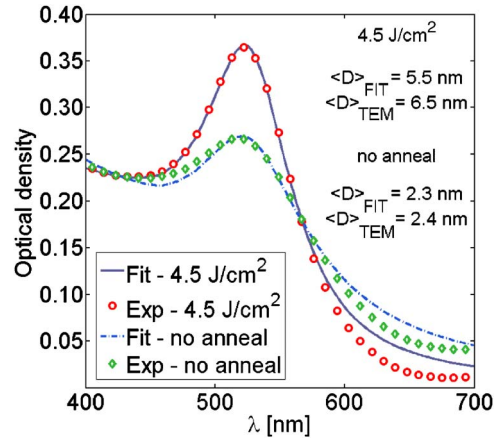

FIG. 3. (Color online) Optical absorption spectra of as-implanted and 4.5 J/cm^2 pulsed laser annealed sample. The dot-dashed and full lines represent the respective nonlinear fits. The average cluster diameter obtained from the fit is compared to the STEM extracted average diameter.

was calculated using the Mie theory with a finite-size correction to the Au bulk dielectric function.[19] $f(R)$ was assumed to be a log-normal distribution function. Figure 3 shows the optical spectra of the two STEM analyzed samples along with the corresponding nonlinear fits. The average cluster diameter that was extracted from the fitting process is $\langle D\rangle = 2.3$ nm for the as-implanted sample and $\langle D\rangle = 5.5$ nm for the laser annealed sample. These values correlate well with the STEM data. The slight discrepancy between the experimental and fitted average cluster diameters for the laser annealed sample could be caused by the fact that the size distribution [Fig. 2(b)] does not exactly have log-normal shape. However, when we fit the optical spectra using a normal distribution, the extracted average cluster diameter $\langle D\rangle = 5.6$ nm is essentially the same as that for the log-normal distribution fit.

IV. CONCLUSION

The results of Fig. 2 demonstrate that the IR laser radiation results in the growth of the Au nanoparticles with a narrowing of the size distribution in a region whose size and depth can be precisely controlled by laser parameters. The results of Fig. 1 demonstrate that this process produces a pronounced effect on the optical properties and is expected to produce a similar significant effect on the nonlinear optical properties of these composites. The rapidity of the annealing process, the lack of atmosphere dependence, the ability to spatially localize the annealing effect, and the existence of the broad IR absorption wavelength region for many optical substrates are the advantages that can make the IR pulsed laser annealing a useful tool in processing the nanocomposite optical materials.

ACKNOWLEDGMENTS

This work was supported in part by the Medical Free-Electron Laser Program of the Department of Defense under Contract No. F49620-01-1-0429, by the National Science Foundation GOALI Grant No. DMR-0513048, by the U.S. Department of Energy Grant No. DE-FG02-01ER45916, and

Downloaded 15 Aug 2008 to 160.91.172.37. Redistribution subject to AIP license or copyright; see http://jap.aip.org/jap/copyright.jsp

by the McMinn Endowment at Vanderbilt University. S.J.P. acknowledges the support from the Division of Materials Sciences and Engineering, the U.S. Department of Energy under the contract with UT-Battelle.

[1]R. F. Haglund, Jr., Mater. Sci. Eng., A **253**, 275 (1998).
[2]J. C. Pivin, Mater. Sci. Eng., A **293**, 30 (2000).
[3]G. Battaglin, V. Bello, E. Cattaruzza, F. Gonella, G. Mattei, P. Mazzoldi, R. Polloni, C. Sada, and B. F. Scremin, J. Non-Cryst. Solids **345**, 689 (2004).
[4]G. Battaglin, E. Cattaruzza, F. Gonella, R. Pollini, F. D'Acapito, S. Colonna, G. Mattei, C. Maurizio, P. Mazzoldi, S. Padovani, C. Sada, A. Quaranta, and A. Longo, Nucl. Instrum. Methods Phys. Res. B **200**, 185 (2003).
[5]G. Battaglin, E. Cattaruzza, C. D. Fernandez, G. De Marchi, F. Gonella, G. Mattei, C. Maurizio, P. Mazzoldi, A. Miotello, C. Sada, and F. D'Acapito, Nucl. Instrum. Methods Phys. Res. B **175**, 410 (2001).
[6]P. Huber, H. Karl, and B. Stritzker, Appl. Phys. Lett. **88**, 203123 (2006).
[7]A. Halabica, R. H. Magruder III, and R. F. Haglund, Jr., Proc. SPIE **6458**, 645810 (2007).
[8]I. Okur and P. D. Townsend, Nucl. Instrum. Methods Phys. Res. B **222**, 583 (2004).
[9]A. L. Stepanov, Tech. Phys. **50**, 285 (2005).
[10]P. Townsend and J. Olivares, Appl. Surf. Sci. **109**, 275 (1997).
[11]R. A. Wood, P. D. Townsend, N. D. Skelland, D. E. Hole, J. Barton, and C. N. Afonso, J. Appl. Phys. **74**, 5754 (1993).
[12]A. L. Stepanov, D. E. Hole, A. A. Bukharaev, P. D. Townsend, and N. I. Nurgazizov, Appl. Surf. Sci. **136**, 298 (1998).
[13]A. L. Stepanov, Rev. Adv. Mater. Sci. **4**, 123 (2003).
[14]D. R. Ermer, M. R. Papantonakis, M. Baltz-Knorr, D. Nakazawa, and R. F. Haglund Jr., Appl. Phys. A: Mater. Sci. Process. **70**, 633 (2000).
[15]R. F. Haglund Jr. and D. R. Ermer, Appl. Surf. Sci. **168**, 258 (2000).
[16]G. S. Edwards, D. Evertson, W. Gabella, R. Grant, T. L. King, J. Kozub, M. Mendenhall, J. Shen, R. Shores, S. Storms, and R. H. Traeger, IEEE J. Quantum Electron. **2**, 810 (1996).
[17]A. Miotello, G. De Marchi, G. Mattei, P. Mazzoldi, and C. Sada, Phys. Rev. B **63**, 075409 (2001).
[18]R. Kofman, P. Cheyssac, A. Aouaj, Y. Lereah, G. Deutscher, T. Bendavid, J. M. Penisson, and A. Bourret, Surf. Sci. **303**, 231 (1994).
[19]U. Kreibig and M. Vollmer, *Optical Properties of Metal Nanoparticles*, Springer Series in Materials Science (Springer-Verlag, Berlin, 1995).
[20]P. Klocek, *Handbook of Infrared Optical Materials*, Optical Engineering Series (Dekker, New York, 1991).
[21]W.-K. Chu, J. W. Mayer, and M. Nicolet, *Backscattering Spectrometry* (Academic, New York, 1978).
[22]D. R. Collins, D. K. Schroder, and C. T. Sah, Appl. Phys. Lett. **8**, 323 (1966).
[23]G. De Marchi, G. Mattei, P. Mazzoldi, C. Sada, and A. Miotello, J. Appl. Phys. **92**, 4249 (2002).

Downloaded 15 Aug 2008 to 160.91.172.37. Redistribution subject to AIP license or copyright; see http://jap.aip.org/jap/copyright.jsp